



## A comparison of metal attenuation in mine residue and overburden material from an abandoned copper mine

D. B. Levy\*

Shepherd Miller, Inc., 3801 Automation Way, Suite 100, Fort Collins CO 80525, U.S.A.

K. H. Custis

Office of Mine Reclamation, Department of Conservation, 801 K Street, Sacramento CA 95814, U.S.A.

W. H. Casey

Department of Land, Air, and Water Resources and Department of Geology, University of California, Davis CA 95616, U.S.A.

and

P. A. Rock

Department of Chemistry, University of California, Davis CA 95616, U.S.A.

(Received 9 March 1996; accepted in revised form 23 August 1996)

**Abstract**—The metal attenuation capacities of secondary acid mine water precipitates is dependent upon such factors as pH, ionic strength, the presence of competing ions, and tailings mineralogy. At the abandoned Spenceville Cu mine in Nevada County, California, approximately 6800 m<sup>3</sup> of jarosite overburden and 28,000 m<sup>3</sup> of hematite residue are potential sources of heavy metals loading to infiltrating surface waters. A column study was performed to assess the ability of the overburden and the residue to attenuate heavy metals from acidic mine drainage. The study information was needed as part of a remedial design for the abandoned mine, and was designed to simulate a worst-case scenario to examine the plausibility of backfilling a large open pit with the waste materials. Ten pore volumes of acidic mine drainage were allowed to pass through the materials, and the column effluents were analyzed for dissolved Fe, Al, Ca, Mg, Na, K, Mn, Cu, Zn, Pb and Ni using ICP-AES. The oxidation–reduction potential (*Eh*) was measured with a combination Pt–Ag/AgCl electrode and also calculated from Fe(II) and Fe(III) measurements using the Nernst equation. Ion activities in solution and saturation index (SI) values for various solid phases were calculated using the geochemical speciation model MINTQA2, and mineralogical compositions of fine (< 2 mm) and coarse (> 2 mm) fractions were determined by XRD. Geochemical modeling of the column effluent compositions indicate that goethite, jarosite, jurbanite and gypsum are potential solid phases that may control metal solubilities in the column effluents. Excellent agreement was observed between the measured *Eh* values and those calculated from the activity ratio of Fe<sup>2+</sup>(aq) to Fe<sup>3+</sup>(aq). The large attenuation capacities for Cu and Zn exhibited by the jarosite overburden also suggest that solid solution substitution plays a large role in controlling metal concentrations in the pore waters. Relatively little metal attenuation, however, was provided by the hematite residue. © 1997 Elsevier Science Ltd. All rights reserved

### INTRODUCTION

Extraction of metals from sulfide ores commonly results in 90% of the minerals being discarded as tailings (Moore and Luoma, 1990). Tailings and associated overburden materials often contain elevated concentrations of potentially toxic metals (e.g., Cu, Zn, Cd and Pb) and are a potential source of localized ground and surface water contamination. As the metals are transported away from their source, their concentrations in surface and ground waters may be controlled by precipitation–dissolution and coprecipitation reactions, adsorption–desorption reactions,

and solid–solution substitutions (e.g., Blowes and Jambor, 1990; Anderson *et al.*, 1991). The extent of metal removal by these processes, however, depends upon a number of factors, including solution pH, ionic strength, the presence or absence of competing cations, and mineralogy of the tailings. From a remediation standpoint, natural attenuation of metals may be preferable to engineered containment methods in materials that have demonstrated a large metals attenuation capacity (Hutchinson and Ellison, 1992). Thus, it is important to consider tailings mineralogy when assessing the potential for metals mobilization from waste-rock materials.

Weathering of pyrite-rich tailings and overburden materials may form a complex assemblage of secondary minerals. In the initial stages of pyrite oxidation, the soluble, hydrated FeSO<sub>4</sub> minerals such as melan-

\* Correspondence address: 3801 Automation Way, Suite 100, Fort Collins, CO 80525, U.S.A.

terite ( $\text{FeSO}_4 \cdot 7\text{H}_2\text{O}$ ), and the mixed Fe(II)–Fe(III) mineral copiapite ( $\text{Fe}^{\text{II}}\text{Fe}^{\text{III}}(\text{SO}_4)_6(\text{OH})_2 \cdot 20\text{H}_2\text{O}$ ), are the first to precipitate (Alpers *et al.*, 1994a). Continued exposure of these minerals to oxidizing conditions leads to the formation of less soluble  $\text{Fe}_2(\text{SO}_4)_3$ , hydroxide and oxyhydroxide minerals, such as schwertmannite ( $\text{Fe}_8\text{O}_8(\text{OH})_6\text{SO}_4$ ), jarosite ( $\text{KFe}_3(\text{SO}_4)_2(\text{OH})_6$ ), ferrihydrite ( $\text{Fe}(\text{OH})_3$ ) and goethite ( $\alpha\text{-FeOOH}$ ) (Schwertmann and Taylor, 1989; Bigam, 1994). In the weathering sequence described by Nordstrom (1982), continued dehydration of goethite and/or exposure to increasing temperatures eventually results in precipitation of hematite ( $\text{Fe}_2\text{O}_3$ ). The secondary minerals formed in acid-mine environments are obviously important because they may serve as the dominant sink for trace metals; however, they differ in their capacities to coprecipitate and adsorb trace metals (Blowes and Jambor, 1990; Alpers *et al.*, 1994b; Jambor, 1994). Therefore, the stage of weathering and the resulting mineralogical composition plays an important role in the ability of mine tailings to attenuate trace metals from ground water.

Approximately  $28,000 \text{ m}^3$  of abandoned red residue and  $6800 \text{ m}^3$  of yellow overburden material were deposited at the abandoned Spenceville Mine site in Nevada County, California (Fig. 1), where nearly 140,000 t of pyrite ore containing 5% Cu were excavated from adits and a large open pit between 1875 and 1888. The Cu was recovered by roasting of the ore and then leaching of the roasted ore piles with water. The dissolved Cu in the leachate was then

precipitated onto Fe metal sheets, producing a cement containing 80% Cu (Irelan, 1892). The bright red, abandoned residue heaps were later used in the production of red-metallic paint from 1890 to 1897 (Bradley, 1930). A previous study of the abandoned wastes has shown that the red residue is primarily composed of hematite, while the yellow overburden is primarily composed of jarosite (Claassen *et al.*, 1994).

A final remediation plan for the Spenceville Mine is currently being designed. The general approach will involve neutralizing the pit water, backfilling the pit with residue or overburden, grading the site to control surface water flow, and revegetation. An important consideration is the potential for the backfill material to retain or release metals upon exposure to potentially acidic ground water. The objectives of the study presented here were to: (1) examine in more detail the chemical and mineralogical composition of the red residue and yellow overburden material present at the Spenceville Mine, and (2) compare the ability of the two materials to attenuate metals upon exposure to acidic mine drainage. The results from this study will be important when apportioning residue and overburden material for backfill and revegetation purposes in the final remediation plan for the Spenceville Mine. In addition, the presence of the two types of waste materials at the Spenceville Mine provides a unique opportunity to study the attenuation capacity of mine tailings in both the early and late stages of weathering, because the yellow overburden and the red hematite residue were derived from the same ore deposit.

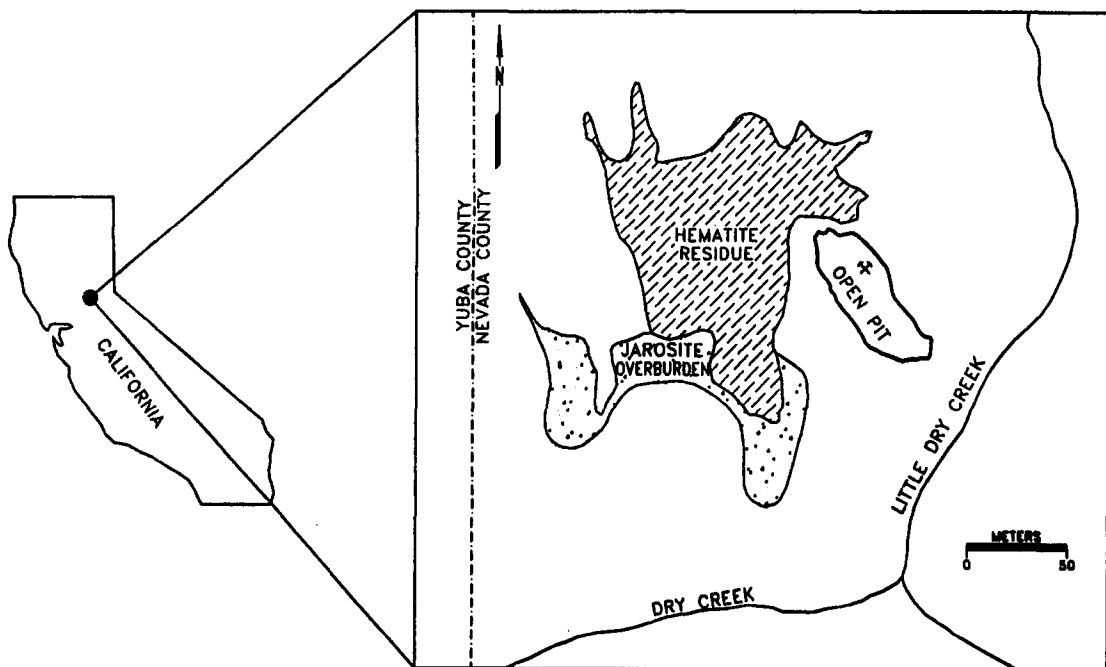


Fig. 1. Location of the Spenceville Mine study area in California.

## MATERIALS AND METHODS

### Collection and preparation of materials

Samples of the acidic pit water, red residue and yellow overburden material were collected from the Spenceville Mine in May 1994. Approximately 80 l of unfiltered water were collected at the surface with a peristaltic pump and placed into polyethylene containers, which were immediately transported to the laboratory and stored in darkness at 4°C. A subsample of the water was filtered through a 0.20 µm pore-size polycarbonate filter and acidified with HNO<sub>3</sub> (pH ≈ 1.0) prior to analysis for dissolved metals. Bulk residue and overburden materials were collected and air dried in the laboratory for 24 h prior to storage in 20 l-capacity polyethylene containers. Subsamples were split into fine (< 2 mm) and coarse (> 2 mm) fractions for chemical and mineralogical analysis by passing the materials through a stainless-steel (2 mm) sieve.

### Chemical analyses of solutions

The filtered Spenceville Pit water that was used as the column influent was analyzed for dissolved Fe, Al, Ca, Mg, Na, K, Mn, Cu, Zn, Pb and Ni using ICP-AES (American Public Health Association (APHA, 1992), and Fe<sup>2+</sup> concentrations were determined by spectrophotometry using the Ferrozine<sup>®</sup> reagent (Gibbs, 1979). The concentration of Fe<sup>3+</sup> was calculated from the difference between total dissolved Fe determined by ICP-AES and Fe<sup>2+</sup> determinations. The concentration of SO<sub>4</sub>-S was determined by the ICP-AES method described by Raue *et al.* (1991). Charge balances for the influent and effluent waters in this study were ≤ 8%. An Orion<sup>®</sup> combination glass/Ag-AgCl electrode was used to measure pH, and the electrical conductivity (EC) was determined with a YSI<sup>®</sup> conductivity bridge and corrected to the standard temperature of 25°C. The oxidation-reduction potential (*Eh*) was measured with an Orion<sup>®</sup> combination Pt/Ag-AgCl electrode, and the value was corrected to a reference standard H electrode by calibration with Zobell solution (APHA, 1992).

Chemical equilibrium calculations were performed using the geochemical speciation model MINTQA2 (U.S. Environmental Protection Agency, 1991) to calculate ion activities and the saturation index (SI) values for various mineral phases. The SI was calculated using the equation:

$$SI = \log(IAP/K_{sp}), \quad (1)$$

where IAP is the ion activity product observed in solution and  $K_{sp}$  is the theoretical solubility constant at the field temperature. Thus, a positive SI indicates that the solution is oversaturated with respect to a given solid phase, while a negative SI indicates undersaturation. A condition of oversaturation indicates that the precipitation of the respective mineral phases is thermodynamically possible. At SI = 0, the solution and solid phases are in equilibrium.

Equilibrium modeling was also used to calculate the system *Eh* from the measured Fe(II) and Fe(III) concentrations with the Nernst equation (Langmuir, 1971):

$$Eh = E^{\circ} + \frac{RT}{nF} \ln \left[ \frac{Fe^{3+}}{Fe^{2+}} \right], \quad (2)$$

where  $E^{\circ}$  is the standard reduction potential (V) of the reaction,  $R$  is the gas constant (8.3144 J K<sup>-1</sup> mol<sup>-1</sup>),  $T$  is the temperature in degrees Kelvin,  $n$  is the number of electrons,  $F$  is Faraday's constant (9.6487 × 10<sup>4</sup> C mol<sup>-1</sup>), and the parameters in brackets represent the activities of Fe<sup>3+</sup>(aq) and Fe<sup>2+</sup>(aq) in solution. The calculated *Eh* values were compared to the *Eh* values measured with the Pt/Ag-AgCl

electrode to test the Nernstian response of the Fe<sup>2+</sup>-Fe<sup>3+</sup> couple in the column effluents.

### Chemical, physical and mineralogical analyses of the solids

Total elemental analysis of the residue and overburden material was achieved by HF digestion in a closed vessel (Lim and Jackson, 1982) followed by analysis of the solutions for Fe, Al, K, Si, Cu, Zn, Pb and SO<sub>4</sub>-S using ICP-AES as described above. The pH was measured on the fine fractions from samples with 1:1 ratios of solid to distilled water (McLean, 1982). A lime requirement determination was performed on the fine fractions by the 4-d Ca(OH)<sub>2</sub> titration described by Sobek *et al.* (1978). Particle density was determined in triplicate using a glass pycnometer method (Blake and Hartge, 1986), and surface area measurements (BET) were determined in triplicate with a Micrometrics<sup>®</sup> Gemini surface area analyzer.

Before and after leaching with the Spenceville Pit water, the mineralogical composition of the residue and overburden was determined on the fine and coarse fractions by preparing them as random powder mounts and analyzing them by X-ray diffraction analysis (XRD) (Moore and Reynolds, 1989). The samples were analyzed with a Scintag XDS-2000 diffractometer using Cu-K<sub>α</sub> radiation with a Ge solid-state detector, and calibrated to better than 0.01 degrees 2θ using a NIST α-Al<sub>2</sub>O<sub>3</sub> (corundum) standard. The samples were run in stepscan mode (0.02°/step) for 1.0 s/step. Mineral phases were identified with XRD by calculating distances between diffraction planes from the recorded diffraction peaks and comparing them with reference standards (Joint Committee on Powder Diffraction Standards, 1993).

### Assembly and leaching of the columns

The leaching columns were constructed from 70 × 5 cm sections of polyvinyl chloride (PVC) conduit, and screened filters were placed at the bottom to prevent the loss of material during leaching and to aid in sample collection. Duplicate columns of residue and overburden material were packed with 50 cm of material to simulate their field bulk densities (1.80 and 1.45 Mg m<sup>-3</sup>, respectively). Porosities were calculated from the measured particle and bulk densities (Hillel, 1982) in order to determine the pore volume of the filled columns. Ten pore volumes of the Spenceville Pit water (influent) flowed through the columns at a rate of approximately 1 cm h<sup>-1</sup>. The column effluent was collected in 750-ml polyethylene containers and immediately filtered through 0.20 µm pore-size polycarbonate filters. The effluent pH, *Eh*, EC and dissolved metal concentrations were determined as described above, and MINTQA2 was used to model the solution composition.

## RESULTS

### Chemical, physical and mineralogical properties

X-ray diffraction analyses of the red residue produced diffraction peaks that correspond to the characteristic d-spacings for hematite (Fe<sub>2</sub>O<sub>3</sub>), quartz (α-SiO<sub>2</sub>) and jarosite (KFe<sub>3</sub>(SO<sub>4</sub>)<sub>2</sub>(OH)<sub>6</sub>), in both the fine and coarse fractions (Fig. 2(a)). The broad band observed in the region of 10–20° 2θ results from the presence of an unidentified, poorly-crystalline solid phase. The XRD results for the yellow overburden

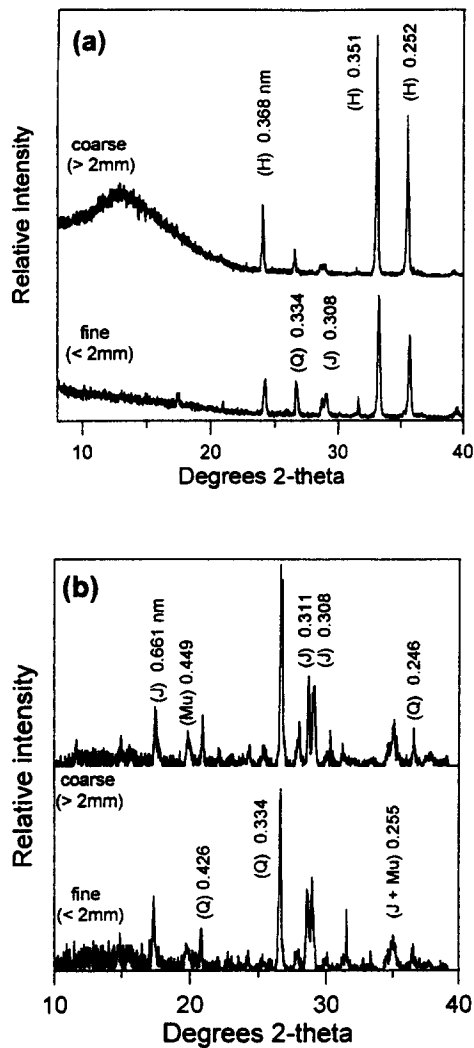


Fig. 2. X-ray diffraction patterns for: (a) the hematite residue, and (b) the jarositic overburden. H = hematite, Q = quartz, J = jarosite, Mu = muscovite.

material also produced characteristic diffraction peaks for jarosite and quartz, but differed from the red residue in that muscovite was also identified and hematite was absent (Fig. 2(b)). The XRD diffraction patterns of both materials after leaching with 10 pore volumes of the Spenceville water were identical to those obtained prior to leaching.

Selected chemical and physical properties of the red residue and yellow overburden are given in Table 1. Both materials had similar 1:1 pH values, and fractions of fine (< 2 mm) and coarse (> 2 mm) particles, although the lime requirement for the residue was significantly lower when compared to the overburden. The hematite material exhibited higher particle densities and much lower surface areas than the jarosite material. The results of the total elemental dissolution are consistent with the results of the XRD analysis. The high concentrations of Fe and Si in the red residue indicate that hematite and quartz are the dominant components (Fig. 2(a)), while the high Al, K, and S concentrations in the yellow overburden are due to higher proportions of jarosite and muscovite (Fig. 2(b)). The concentrations of Cu, Zn and Pb were approximately 3 times higher in the residue than in the overburden material.

#### Chemistry of the hematite residue column effluents

Table 2 shows the results of the chemical analyses for the influent water and the duplicate residue column effluents. Effluent pH values decreased from 2.60 to approximately 2.30, while the EC values increased accordingly. The total dissolved Fe in the influent and effluent waters was predominantly  $\text{Fe}^{3+}$ , and its concentration decreased dramatically as the initial pore volume passed through the column, and remained low for the remainder of the pore volumes. The decrease in concentration was not a result of Fe precipitation during storage of the influent water because visual observations and periodic pH measurements of the influent water provided no indication of Fe precipitation (i.e., precipitates were not visually detected and there was no decrease in pH that could be attributed to ferrihydrite precipitation). Calcium, Mg, Mn, Cu, Zn, Al and  $\text{SO}_4$  behaved conservatively; that is, their concentrations in the column effluent were essentially the same as those in the influent water (Table 2). Sodium, K and Pb concentrations in the effluents exceeded those of the influent water. Representative breakthrough curves for Cu and Zn in the hematite column effluents are shown in Figs 3(a) and 3(b), respectively.

Table 1. Selected chemical and physical properties of the Spenceville mine waste materials

Sample	Chemical properties									Physical properties					
	pH	LR*	Fe	Al	K	S	Si	Cu	Zn	Pb	Bulk density	Particle density	Surface area	% coarse	% fine
			$(\text{g kg}^{-1})$				$(\text{mg kg}^{-1})$			$(\text{Mg m}^{-3})$	$(\text{m}^2 \text{g}^{-1})$	$(> 2 \text{ mm})(< 2 \text{ mm})$			
Hematite	2.8	3.2	690	6.3	4.3	22	148	630	500	850	1.80	4.20	9.69	45	55
Jarosite	2.7	10	120	61	21	40	33	220	150	350	1.45	2.87	33.3	51	49

\* LR = lime requirement = tons of  $\text{CaCO}_3$  per 1000 tons of material required to reach pH = 7.0.

Table 2. Selected chemical properties for the influent water and the duplicate hematite residue column effluents

Pore volume	pH	EC (dS m <sup>-1</sup> )	Fe <sub>T</sub>	Fe <sup>2+</sup>	(μmol l <sup>-1</sup> )					(mmol l <sup>-1</sup> )				
					Mn	Cu	Zn	Pb	K	Al	Mg	Na	Ca	SO <sub>4</sub>
Influent	2.60	3.06	1950	50.0	93.8	403	280	bd <sup>†</sup>	50.4	1.77	3.58	0.80	3.39	15.3
1	2.45	3.64	121	33.1	82.6	390	269	2.12	526	2.23	3.18	1.91	3.34	15.3
2	2.47	3.53	46.4	12.7	84.8	398	267	2.22	414	2.39	3.32	1.33	3.36	16.2
3	2.39	3.64	53.4	14.8	86.2	401	261	2.22	296	2.07	3.37	0.80	3.24	14.6
4	2.37	3.92	72.2	6.44	93.3	382	273	2.46	171	2.01	3.58	0.753	3.36	15.0
5	2.32	4.07	73.2	2.32	92.4	374	278	2.12	128	1.93	3.52	0.731	3.34	16.2
6	2.30	4.16	87.6	0.716	95.1	382	276	2.02	87.9	1.86	3.62	0.748	3.46	15.9
7	2.32	4.19	74.3	2.68	95.9	372	269	1.83	88.7	1.85	3.61	0.775	3.39	15.6
8	2.27	4.31	82.7	0.895	93.7	395	276	1.40	74.6	1.83	3.63	0.775	3.49	16.7
9	2.27	3.94	116	0.895	94.8	393	275	0.869	67.5	2.02	3.70	0.753	3.56	16.3
10	2.24	3.99	260	1.61	92.8	354	278	0.917	89.0	2.05	3.66	0.770	3.46	16.5
1	2.46	3.95	138	38.1	89.0	415	278	1.54	552	2.36	3.40	2.22	3.59	17.8
2	2.47	3.53	59.6	8.41	90.6	399	275	1.59	475	2.40	3.50	1.47	3.41	16.4
3	2.44	3.7	79.0	14.5	90.6	379	266	2.02	271	2.22	3.48	0.975	3.46	15.9
4	2.38	3.8	157	21.3	92.2	327	261	1.59	151	2.10	3.57	0.857	3.39	16.4
5	2.38	3.94	133	5.01	95.3	344	263	1.11	111	1.95	3.57	0.740	3.36	16.0
6	2.37	3.93	157	11.8	95.1	328	292	0.917	92.5	2.07	3.60	0.744	3.41	16.1
7	2.35	4.11	165	3.92	93.0	369	275	0.627	83.1	1.80	3.50	0.770	3.36	16.5
8	2.27	4.27	117	1.25	94.1	372	278	0.676	71.1	1.76	3.56	0.748	3.41	16.0
9	2.25	3.96	175	1.25	97.7	384	282	0.579	39.6	2.02	3.76	0.757	3.51	17.1
10	2.27	3.75	355	4.66	96.6	292	263	0.632	100	2.12	3.62	0.757	3.36	16.4

<sup>†</sup> bd = below detection = 0.50 μmol l<sup>-1</sup> for Pb.

#### Chemistry of the jarosite overburden column effluents

Table 3 shows the results of the chemical analyses for the influent water and the duplicate overburden column effluents. In contrast to the hematite residue, the pH values were higher and the EC values were lower in the jarosite column effluents compared to the influent water. The jarositic overburden also exhibited a much higher attenuation capacity for metals than did the hematite residue. As in the hematite column effluents, the dissolved Fe was predominantly Fe<sup>3+</sup>. Table 3 shows that the concentrations of Fe, Ca, Mg,

Mn, Cu and Zn in the effluent were less than those in the influent in the initial stages of leaching, and then exhibited breakthrough between approximately 6 and 10 pore volumes. Representative breakthrough curves for Cu and Zn in both sets of overburden material are shown in Fig. 3(a) and 3(b), respectively. The Pb concentrations remained below the detectable limit (0.50 μmol l<sup>-1</sup>) in all of the jarositic column effluents. The Al concentrations in the column effluent were generally 1.5–2 times higher than the influent concentrations, while Na and K behaved conservatively in the columns (Table 3).

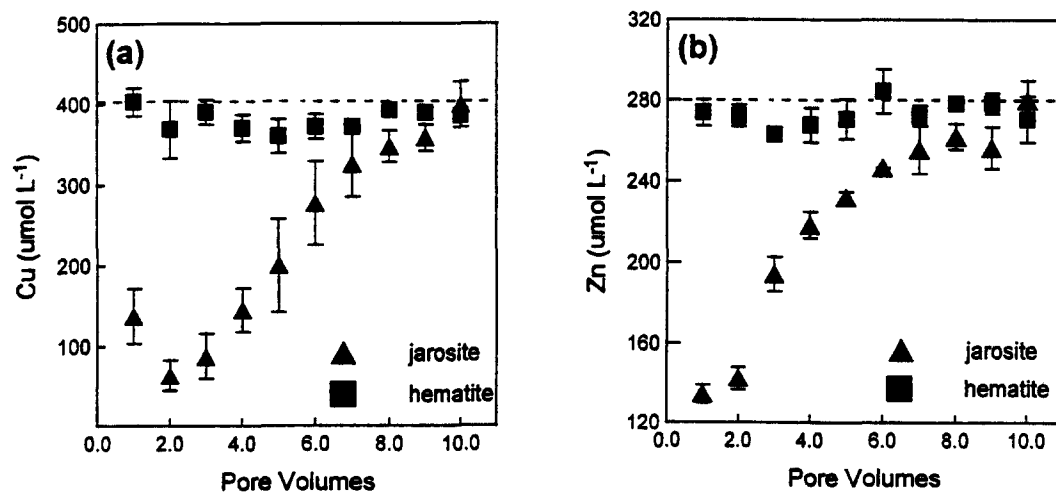


Fig. 3. Representative breakthrough curves for: (a) Cu and (b) Zn in the residue and overburden. Dashed line indicates influent value.

Table 3. Selected chemical properties for the duplicate jarosite overburden column effluents<sup>†</sup>

Pore volume	pH	EC (dS m <sup>-1</sup> )	Fe <sub>T</sub>	Fe <sup>2+</sup>	Mn	Cu	Zn	K	Al	Mg	Na	Ca	SO <sub>4</sub>
			(μmol l <sup>-1</sup> )						(mmol l <sup>-1</sup> )				
Influent	2.60	3.06	1950	50	93.8	403	280	50.4	1.77	3.58	0.80	3.39	15.3
1	2.61	2.38	202	4.30	58.0	162	137	33.5	1.75	1.99	0.883	2.44	10.5
2	2.70	2.38	78.6	8.95	59.3	50.3	137	99.4	4.11	1.86	0.740	2.57	14.4
3	2.75	2.41	50.5	8.95	79.9	67.6	215	85.1	3.89	2.73	0.718	2.57	15.1
4	2.77	2.49	38.1	2.15	87.9	163	233	86.4	3.81	3.12	0.727	2.89	15.3
5	2.77	2.52	33.3	6.45	90.8	262	233	73.9	3.59	3.41	0.740	3.14	15.5
6	2.72	2.71	31.0	3.40	91.1	313	246	54.4	3.22	3.20	0.722	2.99	15.1
7	2.66	nm <sup>‡</sup>	35.3	4.66	93.7	354	247	54.2	3.09	3.32	0.740	2.96	14.6
8	2.66	2.67	31.0	2.15	102.1	360	258	36.8	3.66	3.75	0.714	3.36	16.2
9	2.66	2.66	29.0	0.537	102.4	369	264	32.7	3.32	3.61	0.705	3.31	15.6
10	2.66	nm	28.1	0.179	102.6	379	273	68.5	3.52	3.88	0.775	3.51	16.2
1	2.77	2.26	83.6	4.29	52.2	113	131	59.3	2.59	1.77	0.879	2.37	11.3
2	2.78	2.28	43.9	4.47	53.3	77	146	75.7	2.90	1.79	0.836	2.32	11.6
3	2.78	2.3	41.0	4.48	66.8	107	172	61.1	3.89	2.46	0.862	2.84	14.2
4	2.75	2.44	77.5	2.15	77.9	125	203	63.6	4.15	2.77	0.748	2.96	16.0
5	2.76	2.48	31.3	3.22	87.9	136	230	60.3	3.96	3.11	0.740	2.89	15.9
6	2.71	2.55	30.4	3.94	88.8	240	246	45.7	3.52	3.35	0.753	3.04	15.4
7	2.66	2.57	27.8	4.12	100.4	297	264	45.2	3.74	3.71	0.753	3.29	16.5
8	2.77	2.48	24.5	2.87	104.8	333	266	39.9	3.92	3.73	0.740	3.41	16.6
9	2.72	2.52	27.0	0.895	101.5	346	249	25.3	3.44	3.65	0.735	3.31	15.7
10	2.78	2.54	23.8	0.179	104.8	420	287	30.6	3.78	3.74	0.735	3.54	16.4

<sup>†</sup>Pb was below detectable levels (0.50 μmol l<sup>-1</sup>) in all samples.

<sup>‡</sup>nm = not measured.

### Geochemical modeling

The SI values calculated by MINTEQA2 for goethite (α-FeOOH), jurbanite (AlOH<sub>2</sub>SO<sub>4</sub>), jarosite and gypsum (CaSO<sub>4</sub>·2H<sub>2</sub>O) in the column effluents are shown as a function of pore volume in Fig. 4. The SI values for goethite rapidly decreased from an influent value of +2.8 and approached values of approximately +1.0 in all column effluents (Fig. 4(a)), reflecting the large decrease in Fe concentrations that were observed (Tables 2 and 3). The hematite column effluents remained undersaturated with respect to jurbanite, at values close to the influent value of -0.38, while the jarosite column effluents indicated near-equilibrium conditions with respect to jurbanite (Fig. 4(b)). High degrees of jarosite oversaturation were observed in all the column effluents (Fig. 4(c)), but were significantly lower than that of the influent water (SI = 7.8), again reflecting the loss of Fe from solution that was observed. The SI values for alunite (KAl<sub>3</sub>(SO<sub>4</sub>)<sub>2</sub>(OH)<sub>6</sub>) and alunogen (Al<sub>2</sub>(SO<sub>4</sub>)<sub>3</sub>·17H<sub>2</sub>O) (not shown) indicated that the influent water and all of the column effluents were significantly undersaturated with respect to these minerals. Although slight gypsum undersaturation was observed for the influent water and the hematite column effluents (Fig. 4(d)), the slight undersaturation is probably not significant due to uncertainties in the thermodynamic data. The gypsum SI value in the jarosite column effluents equaled that of the influent

water after 5 pore volumes had passed through the columns.

Excellent agreement was obtained between the *Eh* values measured with the Pt/Ag-AgCl electrode and those calculated from Fe(II) and Fe(III) activities using the Nernst equation (Fig. 5). The solid line in Fig. 5 represents perfect agreement between the measured and calculated *Eh* values. 89% of the values lie within ±30 mV of the solid line, an accepted uncertainty for *Eh* measurements in acid-mine waters (Nordstrom *et al.*, 1979), and 25% of the values were within the measured precision of the Pt electrode (±5 mV). The measured *Eh* values in all of the column effluents ranged from 710 to 810 mV.

### DISCUSSION

The hematite residue and the jarosite overburden have distinctly different abilities to attenuate metals from acidic mine water. The two materials exhibit similar 1:1 pH values and particle size distributions; however, the jarositic overburden material is much more chemically reactive in comparison to the hematite residue. The very low attenuation capacities of the hematite residue result from low surface areas, coupled with the inherently low adsorption affinities of the hematite surface at the pH values encountered (McKenzie, 1980; Schwertmann and Taylor, 1989). Chemical analyses of the hematite column effluents

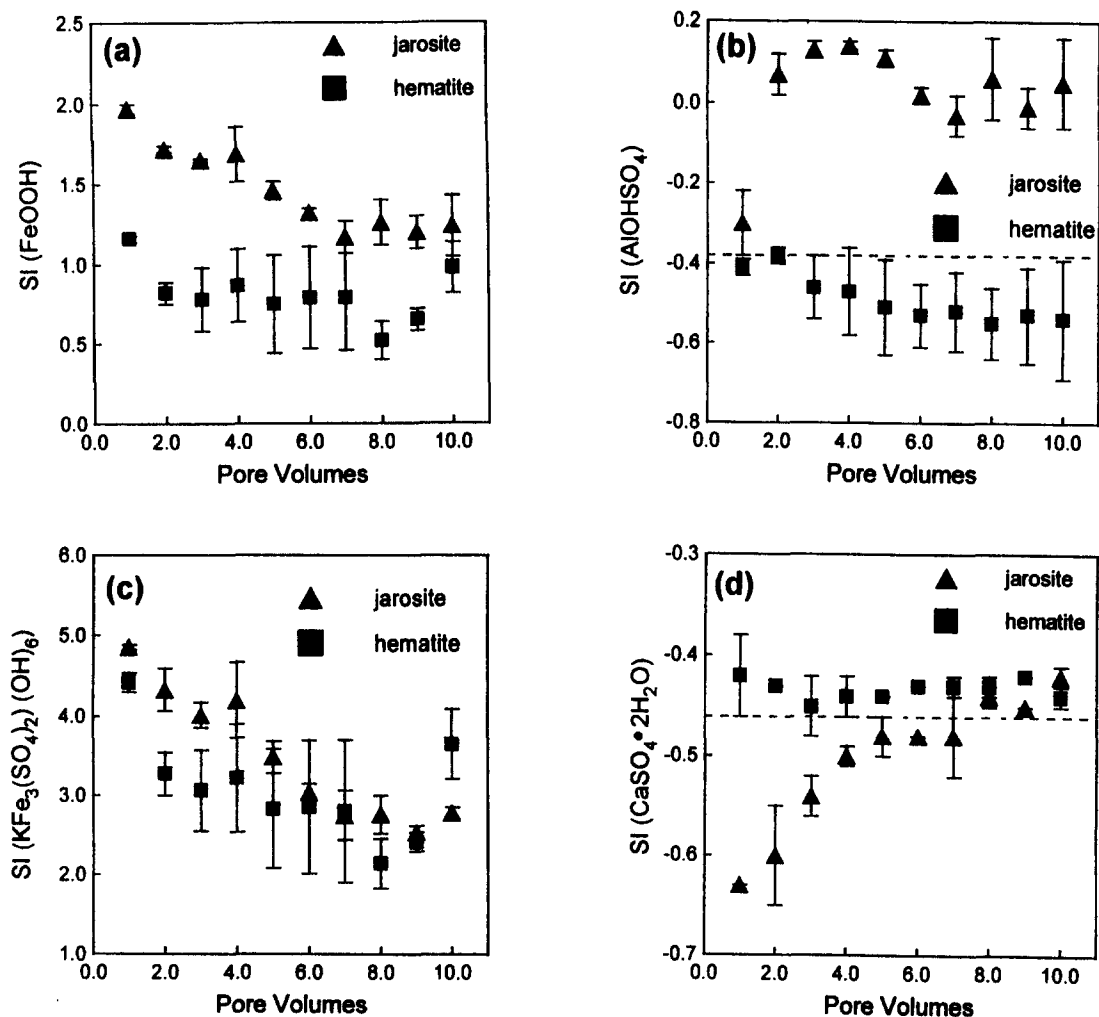
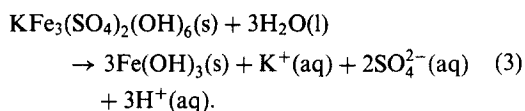


Fig. 4. Saturation index (SI) values calculated for the hematite and jarosite column effluents. (a) Goethite ( $\alpha$ -FeOOH), (b) jurbanite ( $\text{AlOHSO}_4$ ), (c) K-jarosite ( $\text{KFe}_3(\text{SO}_4)_2(\text{OH})_6$ ) and (d) gypsum ( $\text{CaSO}_4 \cdot 2\text{H}_2\text{O}$ ). Dashed line indicates influent value where shown. The influent SI value for goethite was +2.8 and the value for jarosite was +7.8.

indicate that this material would be a potential source of Na, K and Pb to percolating ground water that comes into contact with wall rock if used as backfill in the Spenceville Pit. The chemical composition of the hematite column effluents were essentially the same as those of the influent water, except that Fe concentrations in the effluents were greatly reduced, most likely a result of ferrihydrite and/or goethite precipitation. Saturation index values calculated for the column effluents indicate that goethite, jurbanite, jarosite and gypsum are potential solid phases that may act to control metals concentrations in the pore waters.

The pH of the jarositic overburden was essentially the same as that of the hematite residue; however, the lime requirement for the jarosite material was approximately 3 times higher than that of the hematite residue. The jarositic overburden precludes hematite as a weathering product of sulfide ores and is capable of releasing acidity as it weathers to form ferrihydrite,

as shown in the following equation (Van Breeman, 1982):



The higher surface area of the jarosite overburden and the ability of jarosite to incorporate a wide variety of metals into the crystal structure resulted in much higher metal attenuation capacities relative to the hematite residue, as indicated by the generally higher metals concentrations in the hematite residue column effluents (see Tables 2 and 3). Minerals in the alunite-jarosite group are capable of incorporating numerous solid-solution elements, such as Pb, Cu, K, Na, Ca and  $\text{H}_3\text{O}$  (Alpers *et al.*, 1994a; Jambor, 1994). Thus, coprecipitation and solid-solution substitutions of these elements into the jarosite structure are the likely mechanisms for removal of metals from the

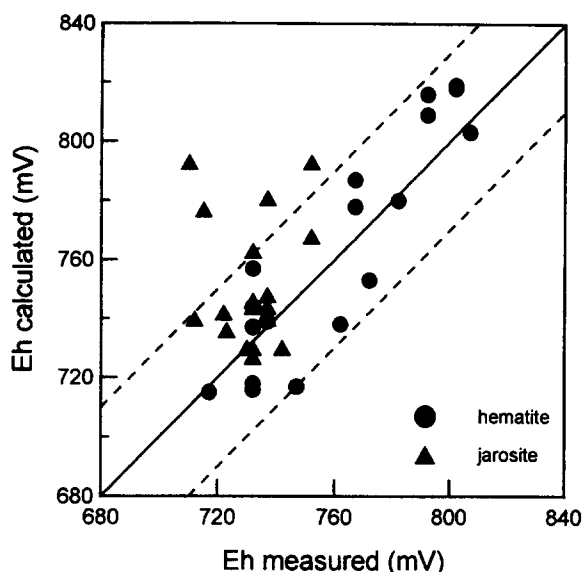


Fig. 5. Calculated versus measured Eh values for the hematite and jarosite column effluents. The solid line represents perfect agreement between the measured Eh and the calculated Eh. The dashed lines represent an uncertainty in the Eh measurement of  $\pm 30$  mV.

jarositic overburden column leachates. From a metals attenuation standpoint, backfilling of the Spenceville Pit with the jarositic overburden, rather than the hematite residue, would be preferred.

The excellent agreement between measured and calculated Eh values observed in this study (Fig. 5) supports the results of the limited number of studies that indicate that in acidic, Fe-rich waters, the measured Eh and total dissolved Fe concentrations can be used to calculate the activity ratios of  $\text{Fe}^{2+}(\text{aq})$  to  $\text{Fe}^{3+}(\text{aq})$  (see Nordstrom *et al.*, 1979; Ball and Nordstrom, 1985; Davis *et al.*, 1988; Runnells *et al.*, 1993). Consequently, an increasing number of studies are utilizing this method to examine the redox status of Fe in acid-mine waters (Jambor, 1994; Levy *et al.*, 1997). The results shown in Fig. 5 simultaneously validate the accuracy of the Eh measurements and the assumptions of equilibrium used in the application of the model (Nordstrom *et al.*, 1979).

### CONCLUSIONS

The results of this study demonstrate the importance of tailings mineralogy when assessing remedial options for the Spenceville Pit and other disturbed mine sites. Infiltrating surface waters that encounter sulfide minerals in the pit wall rock may release acidity and metals, and continue to pose threats to local groundwater quality even after remediation techniques have been implemented. From a geochemical standpoint, the jarosite overburden may be the desired material for use as backfill material in the Spenceville Pit, because use of this material would afford a greater degree of metal attenuation until a stable vegetative

cover is established. From an overall remediation perspective, however, other factors, such as the suitability of waste materials to support revegetation efforts, should also be considered.

*Acknowledgements*—This research was funded, in part, by grants from the California Department of Conservation, Interagency Agreement No. 4093-529, and from the National Science Foundation (EAR 9302069). The authors greatly appreciate the comments provided by Dr R.J. Bowell, Dr R. Fuge, Dr D.D. Runnells, and W.C. Bennett. Also thanks to Jason Fegley for preparing Fig. 1.

*Editorial handling:* R. Fuge.

### REFERENCES

- Alpers C. N., Blowes D. W., Nordstrom D. K. and Jambor J. L. (1994a) Secondary minerals and acid mine-water chemistry. In *The Environmental Chemistry of Sulfide Mine Wastes* (eds. D. W. Blowes and J. L. Jambor), pp. 247–270. Mineralogical Association of Canada, Waterloo, Ontario.
- Alpers C. A., Nordstrom D. K. and Thompson J. M. (1994b) Seasonal variations of Zn/Cu ratios in acid mine water from Iron Mountain, California. In *Environmental Geochemistry of Sulfide Oxidation* (eds. C. N. Alpers and D. W. Blowes), pp. 324–344. ACS Symposium Series 550. American Chemical Society, Washington, D.C.
- American Public Health Association (1992) Standard Methods for the Examination of Water and Wastewater. 18th ed. Am. Public Health Assoc., Washington, D.C.
- Anderson M.A., Bertsch P.M., Feldman S.B. and Zelazny L.W. (1991) Interactions of acidic, metal-rich coal pile runoff with a subsoil. *Environ. Sci. Technol.* **25**, 2038–2046.
- Ball J. W. and Nordstrom D. K. (1985) Major and trace element analyses of acid mine waters in the Leviathan

- mine drainage basin, California/Nevada—October 1981 to October 1982. U.S. Geol. Surv. Water Resour. Invest. Rept. 85-4169.
- Bigham J. M. (1994) Mineralogy of ochre deposits formed by sulfide oxidation. In *The Environmental Chemistry of Sulfide Mine Wastes* (eds. D. W. Blowes and J. L. Jambor), pp. 103–132. Mineralogical Association of Canada, Waterloo, Ontario.
- Blake G. B. and Hartge K. H. (1986) Particle density. In *Methods of Soil Analysis, Part 1* (ed. A. Klute), pp. 377–381. ASA, SSSA, Madison, WI.
- Blowes D.W. and Jambor J.L. (1990) The pore-water geochemistry and the mineralogy of the vadose zone of sulfide tailings, Waite Amulet, Quebec, Canada. *Appl. Geochem.* **5**, 327–346.
- Bradley W. W. (1930) Report XXVII of the State Mineralogist. California Division of Mines. California State Printing Office, Sacramento, California.
- Claassen V., Borch R. and Hastings L. (1994) Analysis of amendments required for revegetation of the Spenceville Mine. Interim report submitted to Office of Mine Reclamation, California Department of Conservation, Sacramento, California. Interagency Agreement Contract No. 1093.
- Davis A. O., Chappel R. and Olsen R. L. (1988) The use and abuse of *Eh* measurements: are they meaningful in natural waters? *Proc. Ground Water Geochemistry Conference*. pp. 97–106. Nat. Water Well Ass. Dublin, Ohio.
- Gibbs M.M. (1979) A simple method for the rapid determination of iron in natural waters. *Water Research* **13**, 295–297.
- Hillel D. (1982) *Introduction to Soil Physics*, Academic Press, San Diego, California.
- Hutchinson I. P. G. and Ellison R. D. (1992) *Mine Waste Management*, Lewis Publishers, Boca Raton, Florida.
- Irelan W., Jr (1892) Eleventh Report of the State Mineralogist, pp. 313–314, California State Mining Bureau.
- Jambor J. L. (1994) Mineralogy of sulfide-rich tailings and their oxidation products. In *The Environmental Chemistry of Sulfide Mine Wastes* (eds. D. W. Blowes and J. L. Jambor), pp. 59–102, Mineralogical Association of Canada, Waterloo, Ontario.
- Joint Committee on Powder Diffraction Standards (1993) *Mineral Powder Diffraction File Databook*, JCPDS, Swarthmore, PA.
- Langmuir D. (1971) *Eh*-pH determination. In *Sedimentary Petrology* (ed. R. E. Carver), pp. 597–634, John Wiley and Sons, New York.
- Levy D. B., Custis K. H., Casey W. H. and Rock P. A. (1997) The aqueous geochemistry of the abandoned Spenceville Copper Pit, Nevada County, California, *J. Environ. Qual.* **26**, 233–243.
- Lim C. H. and Jackson M. L. (1982) Dissolution for total elemental analysis. In *Methods of Soil Analysis. Part 2* (eds. A. L. Page *et al.*), pp. 1–12, ASA, SSSA, Madison, WI.
- McKenzie R.M. (1980) The adsorption of lead and other heavy metals on oxides of manganese and iron. *Aust. J. Soil Res.* **18**, 61–73.
- McLean E. O. (1982) Soil pH and lime requirement. In *Methods of Soil Analysis. Part 2* (eds. A. L. Page *et al.*), pp. 199–224, ASA, SSSA, Madison, WI.
- Moore J.N. and Luoma S.N. (1990) Hazardous wastes from large-scale metal extraction. *Environ. Sci. Technol.* **24**, 1278–1285.
- Moore D. M. and Reynolds R. C., Jr (1989) *X-ray Diffraction and the Identification and Analysis of Clay Minerals*. 332 pp, Oxford University Press, New York.
- Nordstrom D. K. (1982) Aqueous pyrite oxidation and the consequent formation of secondary iron minerals. In *Acid Sulfate Weathering* (eds. J. A. Kittrick, D. S. Fanning and L. R. Hossner), pp. 37–56, SSSA Spec. Publ. 10. SSSA, Madison, WI.
- Nordstrom D. K., Jenne E. A. and Ball J. W. (1979) Redox equilibria of iron in acid mine waters. In *Chemical Modeling in Aqueous Systems* (ed. E. A. Jenne), pp. 51–79, ACS Symposium Series 93. American Chemical Society, Washington, D.C.
- Raue B., Brauch H.J. and Frimmel F.H. (1991) Determination of sulphate in natural waters by ICP/OES—comparative studies with ion chromatography. *Fresenius J. Anal. Chem.* **340**, 395–398.
- Runnells D. D., Skoda, R. E., Kempton J. H., Lindberg R. D. and Bright D. A. (1993) Redox chemistry of aqueous arsenic, selenium and iron with applications to equilibrium geochemical modeling. Prepared for Electric Power Research Institute, Palo Alto, California by the Department of Geological Sciences, University of Colorado, Boulder, Colorado.
- Schwertmann U. and Taylor R. M. (1989) Iron Oxides. In *Minerals in Soil Environments* (eds. J. B. Dixon and S. B. Weed), pp. 379–427, Soil Science Society of America, Madison, WI.
- Sobek A. A., Schuller W. A., Freeman, J. R. and Smith R. M. (1978) Field and Laboratory Methods Applicable to Overburdens and Minesoils., Office of Research and Development, USEPA, Cincinnati, OH.
- U.S. Environmental Protection Agency (1991) MINTEQA2/PRODEFA2, a geochemical assessment model for environmental systems: Version 3.0 users manual, U.S.E.P.A. Rep. 600/3-91/021. Center for Exposure Assessment and Modeling, Office of Res. and Dev., Environ. Res. Lab, Athens, GA.
- Van Breeman N. (1982) Genesis, morphology, and classification of acid sulfate soils in coastal plains. In *Acid Sulfate Weathering* (eds. J. A. Kittrick, D. S. Fanning and L. R. Hossner) pp. 95–108, SSSA Spec. Publ. 10. SSSA, Madison, WI.